Sulfuric Acid Mist Generation in Utility Boiler Flue Gas

3.4.03 Wayne Buckley, VP General Manager, Croll-Reynolds Clean Air Technologies, Inc.
Boris Altshuler, Senior Process Engineer, Croll-Reynolds Clean Air Technologies, Inc.

Sulfur Dioxide (SO_2), Sulfur Trioxide (SO_3) and Oxides of Nitrogen, mainly NO and NO_2, are generated during the combustion of certain fossil fuels. Electric power generating units contribute more than 70% of the national SO_x emissions [1]. When significant volumes of flue gas containing these oxides are discharged to the atmosphere, various state or local authorities set standards for the regulation of these pollutants, since they may impair human health. Sulfur Trioxide (SO_3), which is hydrated to form sulfuric acid (H_2SO_4) from moisture contained in the gas stream or in the atmosphere, may also violate local opacity regulations. Similar opacity problems take place after NO_x removal by both catalytic and non-catalytic reduction processes using ammonia. Ultra-fine particles of ammonium sulfate $(NH_4)_2SO_4$ and sulfite $(NH_4)_2SO_3$ may likewise cause a visible plume. Visibility reduction related to air pollution is caused primarily by 0.1 to 1.0mk diameter particles at a concentration of 1ppm (v) or greater at the stack outlet [2]. While SO_2 emissions can be reduced using commercial Flue Gas Desulfurization (FGD) technology and NO_x emissions can be abated by Selective Catalytic Reduction (SCR) or other processes, the removal of SO_3 and control of aerosol sulfuric acid and ammonia salts is not as straight forward. Depending upon the type of FGD technology utilized, a considerable portion of these aerosols may exit the stack (30 – 60%) as a respirable sub-micron fine particle emission, which presents an extremely difficult air pollution control problem [3]. SO_2 removal technologies may be grouped into the following major categories [4].

˜ Disposable Wet FGD
˜ Disposable Dry FGD
˜ Regenerable Wet and Dry FGD

In disposable technologies, the SO_2 is permanently bound to a sorbent, which must be disposed of as a waste or by-product (e.g. gypsum). In regenerable technologies, the SO_2 is released from the sorbent during a regeneration step and may be further processed to yield sulfuric acid, elemental sulfur or liquid SO_2. The regenerated sorbent is recycled in the SO_2 scrubbing step. For coal-fired electric power plants in the US, approximately 83% utilize wet disposable FGD technologies, 14% dry disposable FGD technologies and the remaining 3% regenerable FGD technologies [1]. Both disposable and regenerable technologies are further classified as wet or dry. In wet processes, wet slurry waste or byproduct is produced and the flue gas leaving the absorber is saturated with moisture. For this process sulfuric acid mist can form instantly after the flue gas is saturated and immediately create stack opacity. In dry processes, dry waste material is produced and the flue gas leaving the absorber is not saturated with moisture. As a rule, dry FGD processes that remove fine particles such as $(NH_4)_2SO_4$, have a low removal efficiency for SO_3 vapors, which later convert at stack conditions to sulfuric acid mist, producing significant visible emissions. This paper presents the mechanisms of fine sulfuric acid mist formation from utility plants in order to develop and implement appropriate air pollution control strategies.

Sulfuric acid formation takes place through the reaction steps of: Oxidation of SO_2 to produce SO_3 (1) followed by reaction with H_2O to form H_2SO_4 (2):

SO_2 + ½ O_2 ? SO_3 (1)

SO_3 + H_2O ? H_2SO_4 (2)

Fig. 1 schematically illustrates the formation of SO_3 in a gas containing SO_2 (1000 ppm) and O_2 (1%) at different temperatures [3]. Since the reaction of SO_2 and O_2 to form SO_3 (Reaction 1) is exothermic, little SO_3 forms at high temperatures (above 1400?C). At 600?C, about 70% of the SO_2 can be converted to SO_3, but the reaction rate is much slower. Under typical conditions of 400?C (750?F), the oxidation of SO_2 to SO_3 is no more than 2% [5]. Most of the SO_3 in boiler flue gas likely forms during the several seconds when the combustion gas cools from 1600-1700?C to about 1000?C. SO_3 generation also increases with rising oxygen concentration in the flue gas (Reaction 1), however, minimizing oxygen in the combustion gas would increase particulate as shown in Fig. 2. Generally, during the combustion process the sulfur, which is present in the fossil fuel, reacts to form about 95 to 97% sulfur dioxide (SO_2) and the remainder sulfur trioxide (SO_3) [6]. SCR technologies may generate an additonal quantity of SO_3 through catalytic conversion of SO_2 to SO_3 even at low temperatures. There are two primary mechanisms of sulfuric acid mist formation. The first mechanism is the reaction between two vapors H_2O and SO_3 (Reaction 2) forming liquid droplets. The second mechanism of mist formation is sulfuric acid vapor condensation in the bulk gas phase by lowering the gas stream temperature beyond the H_2SO_4 dew point. The estimation of sulfuric acid vapor dew point elevation can be made from the ratio of the partial pressure of sulfuric acid and that of water vapor using a graph where the dew point elevation can be read directly (Fig.3) [7]. The dew point of air and pure water vapor may be found in standard tables, and the dew point of the mixture obtained by addition. For example, a flue gas with a 10% (v) of water vapor and 0.01% (v) of sulfuric acid vapor will give:

$$\frac{P_{H2SO4}}{P_{H2O}} = \frac{0.01}{10} 100 = 0.1\%$$

From Fig. 3 the dew point elevation for this ratio is given as 105?C. The dew point for PH_2O = 10% is 45?C (from standard tables) and so the actual dew point temperature of the sulfuric acid vapors is 105 + 45 = 150?C
The second mechanism of mist formation occurs by vapor condensation in the bulk gas phase by reducing the gas stream temperature below the sulfuric acid dew point. It must be noted that, although the dew point of H_2SO_4 under typical conditions is 150 - 180?C, because of uncertainties of bulk phase temperature differences, non-ideal conditions and wall effects, mist formation could occur at gas temperatures as high as 220?C [8]. When a gas stream containing SO_3, H_2SO_4 and H_2O vapor is cooled, H_2SO_4 vapor condenses and SO_3 vapor and H_2O vapor react to form additional H_2SO_4. Very fine submicron mist particles are formed when the gas is cooled faster than the condensable vapor can be removed by mass transfer, i.e. “shock cooling”. The same effect can take place when a dry gas stream containing SO_3 is mixed with a wet gas stream. For this case, rapid mixing of the two gas streams dramatically minimizes the H_2SO_4 droplet size. Test data of fine sulfuric acid mist formation after mixing two gas streams is presented in Table 1 [9]

Table 1

Data	H_2SO_4 Concentration after gas stream mixing, ppm							Condensed H_2SO_4, ppm
	52.6	118.4	197.4	355.3	631.6	736.8	1013.2	36053 (3.6%)
Average diameter of H_2SO_4 droplets, mk	0.028	0.032	0.048	0.056	0.058	0.064	0.062	0.5
oncentration of droplets, $N \cdot 10^{-10}$ per cm^3	---	---	2.6	3.6	3.9	4.6	5.5	0.08

When the H_2SO_4 concentration after mixing ranges from 50 – 200 ppm, the average measured droplet diameter is less than 0.05 mk. But under high concentration of sulfuric acid, where regular condensation and growth of particles take place, the mist droplet size is actually larger. For example at 3.6% concentration of sulfuric acid in the gas phase, the average diameter of mist is 0.5 mk (Table 1). A similar process of mist formation takes place over a surface of high concentration sulfuric acid. At acid strengths below 98.5%, the acid begins to exert a measurable water vapor pressure, which causes submicron mist formation (Fig 4) [8]. The diameter of the formed droplets depends on the equilibrium partial pressure of water. The diameter of the droplet is constant (water vapor pressure 0.06 mm Hg) when the water molecules which vaporize with the sulfuric acid surface are sufficient to react with all of the SO_3 [9]. If the acid mist contacts the water saturated gas stream, the acid droplets grow by absorption of water. As shown in Fig. 5, the largest droplets contain the lowest concentration of sulfuric acid. However, the initial droplet size depends on the relative concentration of water vapors and sulfur trioxide in the gas phase. Table 2 shows the droplet size distribution for sulfuric acid mist emissions at plant producing strong acid, 20% oleum and 32% oleum [10].

Table 2

	Cumulative weight percent smaller than		
Particle Diameter (microns)	Acid Production Only	20% Oleum Production	32% Oleum Production
0.2	--	0.4	3.6
0.4	--	2	16
0.6	1	4.8	30
0.8	7	8	42
1.0	12	11.6	53
1.5	21	48	86.5
2.0	40	84.5	97

Table 2 illustrates that oleum production results in finer particle size distribution than acid production alone (H_2SO_4 < 98.5%) and that the distribution becomes finer with increasing oleum concentration or ratio of SO_3/H_2O. According to aerosol science the saturation ratio of a vapor in a gas can be given by the equality ratio [11].

$$S = \frac{P}{P_T^*} \quad (1)$$

Where P is the partial pressure of the vapor in the gas and P_T^* is the saturation vapor pressure of the vapor over a plane of the liquid at temperature T. When S>1, the gas is said to be super saturated with vapor; when S=1, the gas is saturated; and when S<1 the gas is unsaturated with vapor. The critical dropet size (nucleus or embryo drop size) can be determined by Kelvin's equation [11]

$$d = \frac{4\nu M}{\rho RT \ln S} \quad (2)$$

Where:
S – saturation ratio;
? – surface tension, erg/cm2 or dynes/cm
? – density, grams/cm3
M – molecular weight
T – temperature, ?K

R – universal gas constant, $8.314 \cdot 10^7 erg \cdot K^{-1}, mol^{-1}$

According to Kelvin's equation (2), droplets smaller than the critical size will evaporate. However, if the gas contains a high concentration of monodisperse aerosols smaller than critical size, the lifetime would be longer since the evaporation of small droplets results in increased super saturation, leading to growth of other droplets. Table 3 shows the result of a calculation of critical nucleus droplet size for different sulfuric acid saturation ratios.

Table 3

Saturation ratio, S	Critical drop size, mk
1.1	0.027
1.5	0.0062
2.0	0.0036
3.0	0.0023
4.0	0.0018
5.0	0.0016
10.0	0.0011
15.0	0.0009

The formed nucleus droplets begin to grow and coagulate. For example, according to test data with 3.6% H_2SO_4 condensation (Table 2), the saturation ratio was 5 but the measured size of the condensed mist was 0.5mk while the calculated size is 0.0016mk (Table 3). This indicates that at the test conditions droplet growth and coagulation took place. The measured average diameter of sulfuric acid mist, which was formed by mixing SO_3 and water vapors is about 0.05 mk (Table 2). This value is closer to the critical droplet size because under low H_2SO_4 concentration (maximum 1000ppm) the coagulation and growth processes have a lower rate than at the test conditions. In all the processes where the fog forms, the condensed vapors present in the gas volume and the weight concentration of the fog is proportional to the differential in vapor pressure at the beginning and at the end of the mist formation process. If we assume that at the end of the mist formation process the droplets are large enough and there is an equilibrium between the vapor pressure in gas phase and the saturation vapor pressure over the droplets, the weight concentration of the mist can be approximateed by [9]. $G = \frac{M\left(P - P_T^{*}\right)}{RT} = \frac{MP_T^{*}}{RT}\left(S-1\right)$ (3)

Where:

G – weight mist concentration, gram/cm3 (under normal conditions)

P, - vapor pressure in the beginning of process and saturation vapor pressure under the temperature at the end of condensation, mm.Hg

T – temperature, ?K

S – saturation ratio

R – gas constant, $6.24 \cdot 10^4 \cdot cm^3 .mmHg$

This approximation is correct for most industrial processes, because after the mist formation the super saturation reduces as a result of vapor condensation on the droplets, which have a large surface area. This reduction continues up to equilibrium when the saturation ratio S approaches 1.0. Since the rate of mist formation is very high and total surface of the mist is very large, equation (3) can be used for most practical applications. If the number of formed droplets is N (1/cm^3) the diameter of the droplets is given as $D = 10^{-4}\sqrt[3]{\frac{6M\left(P - P_T^{*}\right)}{\pi \rho RTN}}$ (4)

The maximum rate of critical droplet formation can be calculated by the Frenkel equation [9]

$$I = 10^{26} \cdot \frac{\alpha}{S\rho}\left(\frac{P}{T}\right)^2 \left(M \cdot \sigma\right)^{1/2} \cdot \exp\left(-\frac{17.6 M^2 \sigma^3}{\ell n^2 S \cdot \rho^2 T^3}\right), cm^{-3} \cdot \sec^{-1}$$ (5)

Where α - condensation coefficient (for maximum rate is 1.0)

The number of droplets (N) formed during τ sec is $N = I \cdot \tau \ cm^{-3}$ (6)

The approximately time when the number of droplets achieves a maximum constant value (relaxation time) is given as [9]:

$$\tau = \frac{N}{I} = (I \cdot Ko)^{1/2} = 10^{5} \cdot I^{-1/2}, \text{sec} \quad (7)$$

Where Ko = 10^{-10} (coagulation constant).

As mentioned above, to have condensation take place, sulfuric acid vapor must be supersaturated (S>1). However, sometimes the condensation of sulfuric acid takes place under conditions where it is thermodynamically impossible. As an example, this phenomenon occurs when the flue gas contains fly ash, which may act as a nucleus of condensation for the vapor. In fact fly ash, which is collected in a dry ESP, contains SO_3 which concentrates on the surface of the ash [12] and the smaller fly ash particles have the highest concentration of SO_3 (Table 4) [13]

Table 4

Particle size, mk	SO_3 concentration, % by weight
< 5	0.5
12.3	0.34
> 50	0.13

The SO_3 concentration on the surface of fly ash and the higher concentration of SO_3 on the smallest particles may be explained by direct condensation of sulfuric acid vapors on the fly ash when the flue gas flows through the cooler stages of the APC system. Another mechanism for sulfuric acid condensation under gas phase saturation ratios (S) of less than 1.0 is condensation on colder surfaces. This takes place if the temperature of the equipment walls is significantly lower than the temperature of the gas stream and occurs in the very thin laminar boundary layer of about 20 mk. Since the temperature gradient in this laminar layer is no less than 150?K, the saturation ratio (S) increases up to 10 – 15 [14]. Because the thickness of the laminar layer is a small percentage of the total gas volume, even for heat exchanger surfaces, this mechanism of condensation will not generally provide a considerable quantity of sulfuric acid mist. However, according to Equation (2), the high saturation ratio in this laminar layer may be the mechanism that produces the largest portion of the finest sulfuric acid droplets. For example, after a SCR system, the flue gas temperature is about 250?C and the concentration of sulfuric acid vapor is 50 ppm and therefore the sulfuric acid mist formation ratio is less than 1.0. At these conditions, the gas phase condensation of sulfuric acid has already begun in the laminar layer and, if wall temperature gradient is assumed as 150?K [14], the saturation ratio S will be equal to 10 and the critical droplet size is 0.0011 mk (Table 3). The process of mist formation in the laminar layer may also occur when slow gas quenching takes place, such as through the use of an indirect contact condenser. With a slow cooling process, the presence of fly ash is an important factor because it provides a large surface area on which the vapors can condense [15]. The advantage of this type of cooling is that most of the acid will be condensed on the existing fly ash particles and the condenser walls. However, most FGD systems use rapid quenching technologies with direct contact cooling of the hot flue gas with water. This process inherently generates a large number of sulfuric acid droplets by homogeneous nucleation. The quench rate depends on the temperature gradient and may achieve 10^{8} ?K/sec under high temperatures [16]. When the hot flue gas is quenched from 200 - 250?C (473 - 523?K) to 50?C (323?K) the quench rate is estimated as 2 • 10^{5} ?K/sec with the quench time approximately 1.0 • 10^{-3} sec. For this case the amount of vapor condensation may be estimated using Equation (3). For example, if the inlet quench concentration of sulfuric acid after the SCR is 50 ppm, the sulfuric acid mist loading will be 179 mg/nm^3 (0.078 grain/SCF) after gas quenching. Fig. 6 illustrates the calculated initial droplet size without coagulation of droplets (Curve l) and relaxation time when the coagulation begins (Curve 2 and Equation 7). Under low H_2SO_4 concentration (less saturation ratio S), the average critical droplet size is larger than under high H_2SO_4 concentration. However, the coagulation of mist droplets takes place after a shorter time under high H_2SO_4 concentration. For example, if the initial H_2SO_4 concentration is 10 ppm coagulation begins after 4 sec, but at 40 ppm it has already started after 0.05 sec (Fig. 6). This phenomena may also be illustrated by Table 2. At a high concentration of sulfuric acid (32% oleum production) the particle size distribution of the mist contains small droplets as well as large droplets, which is a result of the coagulation and growth processes. At a lower concentration of sulfuric acid (acid production only) the particle size distribution shows the presence of droplets greater than 0.6mk only (Table 2). If the sulfuric acid condensation process has sufficient time (more than the relaxation time, Equation 7) the droplet size after coagulation and growth is larger for a higher concentration of H_2SO_4 (Table 1). The particle size distribution may be changed by the variation of maximum value of saturation ratio S and of saturation rate $(dS/d\tau)$. For example, in order to increase the droplet diameter it is necessary to reduce the value of $(dS/d\tau)$, S ratio accordingly or reduce the concentration of droplets. The sulfuric acid mist removal efficiency of a conventional FGD system is estimated at 40 – 70% [3]. Fig 7 shows the opacity of the outlet gas for different FGD scrubbing efficiencies. This graph can help to calculate the total efficiency of an FGD system and the additional cleaning equipment necessary to get to near zero visible emissions. For example, if the FGD unit provides 50% sulfuric acid mist removal efficiency, visible emission (greater than 5% opacity) are generated at 7 ppm of H_2SO_4 or higher. In other words, if the inlet to the FGD unit has a concentration of H_2SO_4 of 50 ppm and the FGD has a 50% removal efficiency of H_2SO_4, to get less than 5% opacity at the stack the additional opacity abatement equipment system should have an H_2SO_4 removal efficiency $\frac{25-7}{25} \cong 70\%$. However, this value of efficiency is minimum because at least two other processes take place, which increase opacity. First, when the flue gas enters the FGD scrubber coagulation occurs. The initial high concentration of sulfuric acid mist begins to absorb the water from the saturated gas and the size of the droplets and therefore the weight of mist loading increases. In addition, the final sulfuric acid concentration differs for various droplet sizes (Fig. 4). As an example, a 0.5 mk droplet can absorb about 50%(wt) of water and then the total weight of the mist loading doubles. This would mean that the opacity abatement equipment after the FGD unit should have an efficiency of at least 85% for an inlet concentration of 50 ppm H_2SO_4 . The second consideration is that opacity is a function of not only the concentration of sulfuric acid mist, but also the dust or solid particulate loading. If the flue gas contains solid particulate, a synergetic effect takes place and the opacity increases greater than the proportional increase in combined weight loading of sulfuric acid mist and solid particles. Therefore, an accurate design for an opacity abatement system can only be defined by field testing of the actual FGD system exhaust gas. Flue gas which has passed through a selective catalytic reduction (SCR) system, an air preheater and a dry electrostatic precipitator (DESP) normally ranges between 140 - 160$^{?}$C. After scrubbing in a wet FGD process, the gas temperature usually drops to 55 - 60$^{?}$C. To minimize condensation of acidic liquor, which causes stack corrosion and in some cases acid rain, the flue gas should be reheated to about 80$^{?}$C and to eliminate the formation of any visible plume, the flue gas temperature should be about 140$^{?}$C [3]. Obviously, for large gas flow rates, such as a utility boiler exhaust, gas reheating is very costly and, while reheating can minimize the visible plume caused by sulfuric acid and water vapor, it cannot remove solid particulate or reduce existing acid emissions to satisfy environmental mass emission limits. If reduction of mass emissions, stack opacity or both are required, it is necessary to use a technology that will simultaneously remove both sulfuric acid mist and solid particulate material from the flue gas. Wet Electrostatic Precipitation (WESP) technology can satisfy this requirement and, as proven in numerous industrial applications, has the added potential for abatement of heavy metals (including mercury), as well as water mist carryover from an FGD scrubber system, while minimizing both the capital and operating costs [17]. ***References***

1. *R.K. Srivastava. Controlling SO2 Emissions: A Review of Technologies. EPA/600/R-00/093, Nov. 2000.*
2. *J.F. Mattrey, J.M. Sherer, J.D. Miller. Minimize Emissions from Semiconductor Facilities. Chemical Engineering Progress, May 2000, p.35.*
3. *J. Ando. SO2 Abatement for Stationary Sources in Japan. EPA-600/7-78-210, Nov. 1978, p.82.*
4. *R.K. Srivastava, W. Jozewicz. Flue Gas Desulfurizatio: The State of the Art. J.Air & Waste Management. Assoc., 2001, 5, p.1676.*
5. *H.J. Kim, A. Mizuno, M. Sadakata. Development of a New Dry Desulfurization Process Using TiO2 Catalyst and Non-Thermal Plasma Hybrid Reactor. 7th International Conference on Electrostatic Precipitation. Sept. 20 – 25, 1998, Kyongju, Korea, p.292.*

6. *P.N. Cheremisinoff. Clean Air Pollution Engineering. June 1990, p.66.*
7. *W. Strauss. Industrial Gas Cleaning, Pergamon press Inc., 1975, p.53*
8. *D.R. Duros, E.D. Kennedy. Acid Mist Control. CEP, Sept. 1978, p.70*
9. *A. Amelin. The Theoretical Bases of Fog Formation at the Condensation. Moscow, 1972, p.58 (Russia)*
10. *Control of Sulfuric Acid Mist Emissions from Existing Sulfuric Acid Production Units. ERA Report 450/2-77-019, P.4 –7 (OAQPS No. 1.2 – 078)*
11. *P.C. Reist. Aero Ol Science And Technology, McGrw-Hill, Inc. 1993, p.277.*
12. *L.D. Hlilett, J.A. Carter and others. Trace Element Measurments at the Coal-fired Allen Steam Plant – Particle Characterization. Coal-Utilization Symposium – Focus on SO2 Emission Control, Kentucky, Oct. 22, 1974, p.207*
13. *L.E. Sparks. The onset of Electrical Breakdown in Dust Layers. JAPCA, Nov. 1988, 38, No. 11, p.1412*
14. *A. Gorokhov. Features Sulfuric Acid Condensation from Ash-Laden Waste Gases Colloidal Magazine. No. 2, 1979, p.218 (Russia).*
15. *A.S. Damie, D,S. Ensor, L.E Sparks. Options for Controlling Condensation Aerosols to Meet Opacity Standards. JAPCA, Aug. 1987, 37, No. 8, p. 925.*
16. *L.T. Bucanko, M.G. Kuzmin, L.S. Polak. High Energy Chemistry. Ellis Horwood Limited, 1993, p. 323.*
17. *R. Altman, W. Buckley, I. Ray. Wet Electrostatic Precipitation Demonstrating Promise for Fine Particle Control. Power Engineering, Jan. 2001, p.*

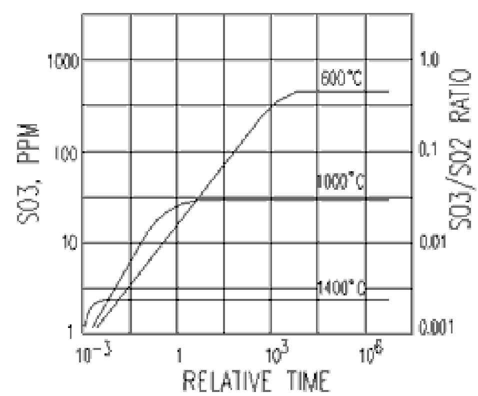

FIG.1

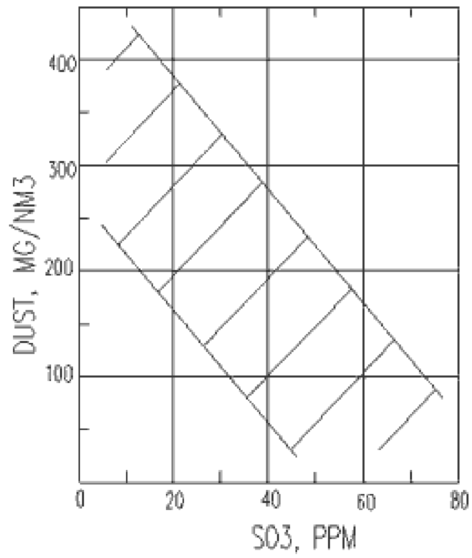
DUST, MG/NM3
400
300
200
100
0
20
40
60
80
SO3, PPM

FIG.2

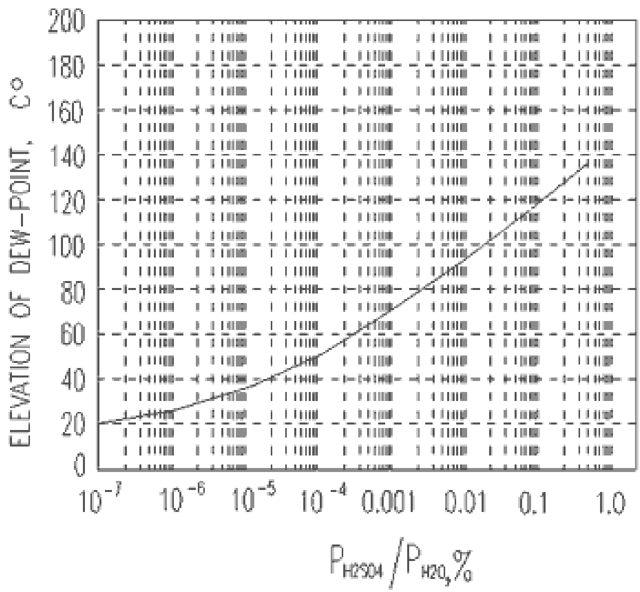
ELEVATION OF DEW-POINT, C°
200
180
160
140
120
100
80
60
40
20
0
10^{-7}
10^{-6}
10^{-5}
10^{-4}
0.001
0.01
0.1
1.0
P_{H2SO4}/P_{H2O},%

FIG.3

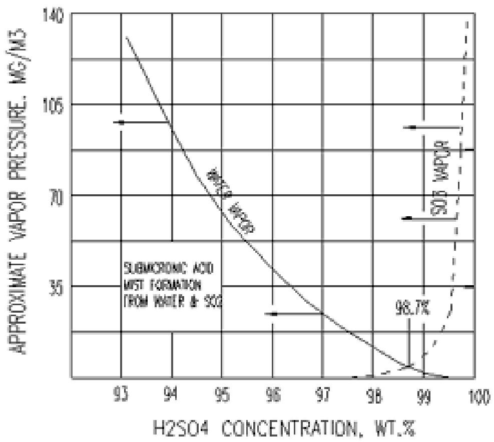
APPROXIMATE VAPOR PRESSURE. MG/M3
140
105
70
35
WATER VAPOR
SO3 VAPOR
SUBMICRONIC ACID MIST FORMATION FROM WATER & SO2
98.7%
93
94
95
96
97
98
99
100
H2SO4 CONCENTRATION. WT.%

FIG.4

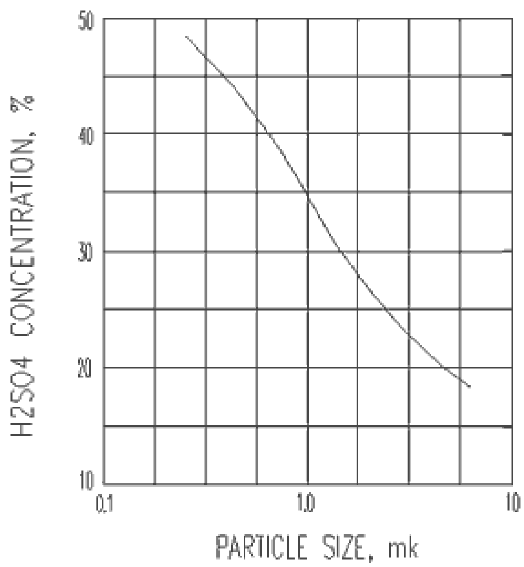
H2SO4 CONCENTRATION, %
50
40
30
20
10
0.1
1.0
10
PARTICLE SIZE, mk

FIG.5

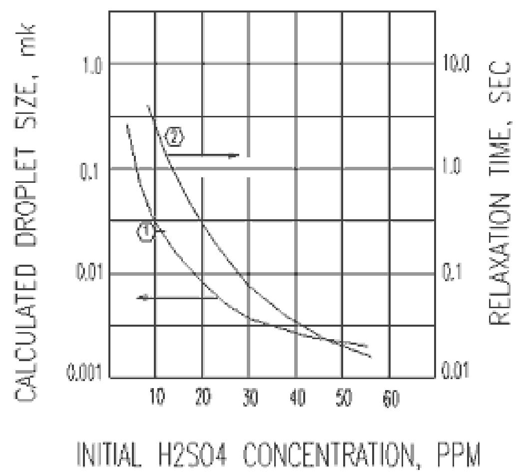

FIG.6

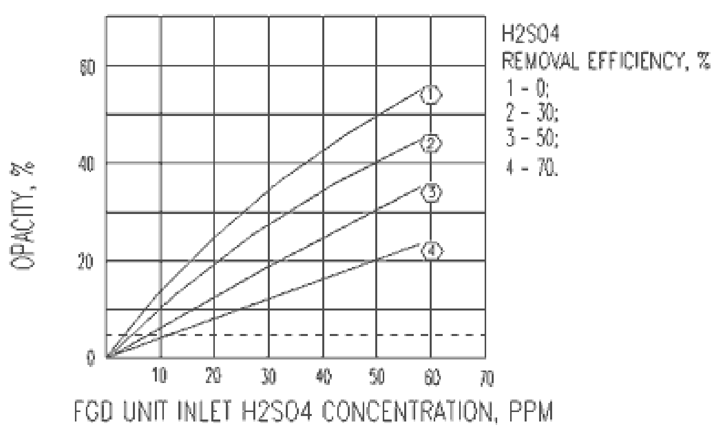

FIG.7

For information on purchasing reprints of this article, contact arowe@reprintbuyer.com.